Radio Synchrotron Emission from Secondary Leptons in the Vicinity of Sgr A*

Roland M. Crocker[1], David Jones[1,2], David R. Ballantyne[3], and Fulvio Melia[3,4,5]

ABSTRACT

A point-like source of ∼TeV γ-rays has recently been seen towards the Galactic center by HESS and other air Čerenkov telescopes. In recent work (Ballantyne *et al.* 2007), we demonstrated that these γ-rays can be attributed to high-energy protons that (i) are accelerated close to the event horizon of the central black hole, Sgr A*, (ii) diffuse out to $\sim$ pc scales, and (iii) finally interact to produce γ-rays. The same hadronic collision processes will necessarily lead to the creation of electrons and positrons. Here we calculate the synchrotron emissivity of these secondary leptons in the same magnetic field configuration through which the initiating protons have been propagated in our model. We compare this emission with the observed $\sim$ GHz radio spectrum of the inner few pc region which we have assembled from archival data and new measurements we have made with the Australia Telescope Compact Array. We find that our model predicts secondary synchrotron emission with a steep slope consistent with the observations but with an overall normalization that is too large by a factor of $\sim$ 2. If we further constrain our theoretical γ-ray curve to obey the implict EGRET upper limit on emission from this region we predict radio emission that is consistent with observations, i.e., the hadronic model of gamma ray emission can, simultaneously and without fine-tuning, also explain essentially all the diffuse radio emission detected from the inner few pc of the Galaxy.

Subject headings: Galaxy: center — radiation mechanisms: nonthermal — gamma rays: theory

[1]School of Chemistry and Physics, The University of Adelaide, Adelaide, South Australia, 5005 Australia; roland.crocker,david.jones@adelaide.edu.au

[2]Australia Telescope National Facility, Marsfield,2122, Australia

[3]Department of Physics, The University of Arizona, 1118 East 4th Street, Tucson, AZ 85721; drb, melia@physics.arizona.edu

[4]Steward Observatory, The University of Arizona, 933 N. Cherry Avenue, Tucson, AZ 85721

[5]Sir Thomas Lyle Fellow and Miegunyah Fellow.

1. Introduction

The Galactic center (GC), at an assumed distance of 7.9 kpc, is a complex region containing many compact and diffuse high-energy astrophysical sources (see Melia 2007 for a recent review). The dynamics of the central few lightyears is dominated by what is believed to be a supermassive black hole, Sagittarius A* (Sgr A*).

The GC has been identified as a point-like source of TeV γ-rays by a number of air Čerenkov telescopes. In our work we concentrate exclusively on the data from HESS (Aharonian *et al.* 2004, 2006b) as these provide the best constraints on the source properties. The GC signal is coincident within $\sim 30''$ of Sgr A*, though with a centroid displaced roughly $7''$ ($\sim$ 0.4 pc) to the East of the GC (Aharonian *et al.* 2004, 2006b). The spectrum is a pure power law with photon index 2.25 ± 0.10, and the total flux above 1 TeV is $(1.87 \pm 0.30) \times 10^{-8}$ m^{-2} s^{-1} (Aharonian *et al.* 2006b).

In a recent paper (Ballantyne *et al.* 2007), we examined a hadronic scenario for the creation of the $\sim$TeV γ-rays: a power-law population of protons is accelerated close to Sgr A*, perhaps through the process of stochastic acceleration on the turbulent magnetic fields expected to pervade this inner region. These then diffuse outwards through the strong magnetic fields of the largely evacuated stellar-wind region surrounding Sgr A* before, finally, colliding with gas in the high molecular density clumps that make up the circumnuclear disk (CND). Such collisions (assumed to be exclusively proton on proton for simplicity) generate neutral mesons that then decay into the γ-rays which, by construction, we detect here at Earth.

In the current work we self-consistently calculate the synchrotron emissivity of the secondary leptons that must also be produced in our scenario. These come from the decay of the charged mesons created in the same p-p collisions that we posit explain the γ-ray emission – though, in constrast to the case for γ-ray emission, we find that, because of the extremely strong magnetic fields there (and despite the relatively low ambient densities) radio emission from the wind region is more important than that from the CND. Finally, we compare our predictions for radio emission with archival and new radio data on the region we have assembled.

2. Proton Propagation

We firstly summarize the results obtained by Ballantyne *et al.* (2007). In our calculation we employed a realistic model of the density of matter through the GC arrived at by Rockefeller *et al.* (2004). These authors computed the density distribution in this region

caused by the interactions of stellar winds from the young stars surrounding Sgr A*. In addition to the stellar wind gas, the volume also contains a high-density torus of molecular gas with an inner radius of 1.2 pc and a thickness of 1 pc representing the observed CND.

The average density in the model stellar-wind gas (taken to be any region where $n_{\rm H} < 3 \times 10^3$ cm^{-3}) is $\langle n_{\rm H}^{\rm sw} \rangle = 121$ cm^{-3}, while it is $\langle n_{\rm H}^{\rm mt} \rangle = 233{,}222$ cm^{-3} within the model molecular torus. Taking $kT = 1.3$ keV as the average temperature of the stellar-wind gas (Baganoff *et al.* 2003; Rockefeller *et al.* 2004), 100 K for the temperature of the molecular torus (Rockefeller *et al.* 2004 and references therein), and assuming equipartition, the average field intensity is 3 mG in the stellar-wind region and 0.35 mG within the torus. In any particular cell the magnetic field was assumed to be generated with an intensity that satisfies $|B| = 1.5 \times 10^{-5}$ Gauss $n_H/10^4$ cm^{-3} for the CND region and $|B| = 2.6 \times 10^{-3}$ Gauss $n_H/10^2$ cm^{-3} in the stellar-wind gas. Our procedure for determining a physical description of the field direction at any position in the computational grid is described in Ballantyne *et al.* (2007).

Computational resources limited our modeling to proton energies between 1 and 100 TeV. A total of 222,617 proton trajectories was calculated with energies uniformly distributed in this range. These trajectories were split into 21 energy bins ($\log(E/{\rm eV}) = [12.0 - 12.1], \ldots, [13.9 - 14.0]$). From these data the steady state distribution of protons (given in cm^{-3} eV $^{-1}$) in each of the 7500 computational cells of the CND and the 7022 cells of the stellar-wind region could be inferred.

As a proton random-walks its way through the the turbulent magnetic field of the GC it may collide with a low-energy proton in the ambient medium and produce pions via the reaction $p + p \rightarrow p + h + N_0\pi^0 + N_\pm\pi^\pm$. Here h, denoting hadron, is a proton or, if charge exchange occurs, a neutron and variable and energy-dependent multiplicities of neutral (N_0) and charged ($N_\pm$) pions are, in general, produced but electric charge must be conserved overall. (In our calculations we also account for the sub-dominant contribution from charged and neutral kaons.) Neutral pions will subsequently decay into two photons and charged pions to electrons, positrons, and neutrinos.

In this Letter we adopt the steady-state proton distributions within each modeled clump of CND and stellar-wind region gas arrived at by Ballantyne *et al.* (2007). We then use the techniques outlined at length in Crocker *et al.* (2007a) to calculate – on the basis of (i) these steady state p distributions, (ii) the ambient hydrogen number density, and (iii) clump magnetic fields – the steady state (processed) distributions of secondary leptons within each clump and the resulting synchrotron emission from each clump.

3. Data

To test our theoretical model we have obtained ∼GHz radio fluxes covering the region of the CND defined by a $2' \times 1'$ rectangle with sides parallel to Galactic longitude/latitude and with Sgr A* at the center. Where possible, we have chosen interferometry data obtained with an array configuration that results in a beam smaller than this region of interest to ameliorate the problem of confusion with nearby strong radio sources (Sgr A East in particular). On the other hand, to ensure that the diffuse flux through this region that we are interested in – present on scales up to the size of the region – is not integrated out, we also demand that the array configuration possess some antenna spacings that are suitably small.

For the reasons just given we make use in our analysis of medium resolution ($\sim 43''$; LaRosa *et al.* (2000)) 330 MHz VLA[1] data, similar resolution SUMSS[2] 843 MHz data, and serendipitous ATCA[3] observations of the GC at 1384 MHz and 2368 MHz. These latter data were obtained with a somewhat lower resolution ($\sim 1' \times 2'$ at 1384 MHz, and $\sim 0.5' \times 1'$ at 2368 MHz.) which is nevertheless sensitive to emission on the size scales of the CND.

For each radio image, we used a number of independent methods to obtain the flux inside the region of interest (see Jones *et al.* (2007) for details). To obtain a conservative estimate on the error in the flux determinations, the standard deviation between all flux estimates at a particular frequency was taken to be the RMS error on the final flux quoted. (Errors due to gain and to image noise make a negligible contribution). The quoted central value for the flux at a given frequency is obtained from smearing the beam to $2' \times 1'$ resolution, and reading the peak flux which provides the most reliable determination.

Flux determinations are: 46 ± 12 Jy at 330 MHz, 37 ± 5 Jy at 843 MHz, 20 ± 6 Jy at 1384 MHz, and 11 ± 2 Jy at 2368 MHz. These data are shown as the lower frequency data points in Figure 1 (b). The data points at 843, 1384, and 2368 MHz define a non-thermal, power-law spectrum in frequency $\propto \nu^{-1.2}$, indicating a steep, synchrotron-radiating electron population (whether primary or secondary) of $\propto E_e^{-3.4}$. The presence of non-thermal emission near Sgr A West was first discussed by Gopal-Krishna & Swarup (1976) and was subsequently extensively investigated by Ekers et al. (1983). We note that the spectrum we determined for the region is steeper than that found by these latter authors though the

[1]The Very Large Array (VLA), as part of the National Radio Astronomy Observatory, is operated by Associated Universities, Inc., under cooperative agreement with the National Science Foundation.

[2]The Molonglo Observatory Synthesis Telescope (MOST) is operated by the University of Sydney

[3]The Australia Telescope Compact Array (ATCA) is operated by the Australia Telescope National Facility, CSIRO, as a National Research Facility.

overall normalization at 1384 MHz is compatible. Our datum at 330 MHz falls below the $E_e^{-3.4}$ power law; this, however, is as expected as Sgr A Complex radio emission is strongly attenuated at around this frequency and below because of free-free absorption by thermal gas associated with the Sgr A West structure as established by Pedlar *et al.* (1989). It is interesting to note that, according to these authors (see also Fatuzzo & Melia (2003)), the spectral index pertaining to Sgr A East as a whole is approximately 1 with a corresponding average flux density at 1384 MHz of approximately 0.014 Jy/arcsec^2. This is roughly half of the flux density we measure from the CND region.

At frequencies higher than 2368 MHz, we have obtained snapshot observations with ATCA at 4800 and 8640 MHz. We measure 22 and 21 Jy at 4800 and 8640 MHz over the same solid angle as for the lower frequency observations and compatible with the results obtained by Brown et al. (1981) at 4.9 GHz. Finally, in Figure 1 (b), we also show fluxes measured by Salter *et al.* (1988) at 84 and 230 GHz, Sofue *et al.* (1986) at 43.25 GHz, and Tsuboi *et al.* (1988) at 91 GHz. These latter measurements are not perfectly matched in solid angle to the region of concern and should be taken as indicative only. Overall, they show that the spectrum of the CND region has become dominated by thermal emission from Sgr A West at $\gtrsim 4$ GHz and do not provide a strong constraint on our secondary synchrotron emission model.

4. Results and Discussion

From the modeling described in Ballantyne *et al.* (2007), we have simulated data describing the steady-state proton distribution for the clumps of matter that make up the CND and the stellar-wind region (each of varying density, magnetic field strength, and position).

Synchrotron radiation in the GHz range by secondary leptons in the mean magnetic field of the CND, 0.35 mG, requires initiating parent p's of energy $\sim 6 \times 10^{10}$ eV and only $\sim 2 \times 10^{10}$ eV in the 3 mG mean field of the wind region (assuming a power-law p spectrum of spectral index 2.3). Such energies are unfortunately well below the 1 TeV threshold of our proton propagation modeling. We assume, then, that the steady-state proton distribution of any given computational cell is a pure power law (in momentum) with such power law fitted to match our modeled 1-100 TeV proton spectra.

Despite our simulating more than 2×10^5 proton trajectories, we must deal (in our power-law fitting) with empty energy bins in many clumps. We address this issue by producing (on the basis of our modeled, *overall* clump spectra) parameterizations of the TeV proton flux and fitted spectral index in terms of the clump radial separation from Sgr A* and magnetic

field strength. With these parameterizations in hand we can determine, for any clump at given radius and with given magnetic field, the *expected* value for the p flux in a given $10^{\rm th}$-decade energy bin. For a zero-entry bin, we replace the zero with this expected value divided by the free parameter X. We then use a MATHEMATICA routine to perform a χ^2 fit in the parameter X of the overall CND TeV γ-ray spectrum to the HESS data (the γ-ray emission by cells in the wind region only contributes at the $\sim 0.1\%$ level and is ignored here).

We find a minimum reduced χ^2 value of 1.2 (for 32 degrees of freedom) at $X = 1.69$. Extension of individual clump spectra below TeV using the power-law assumption then allows us to also make a prediction for the synchrotron radio emission due to secondary leptons in each CND clump and, using the same X value, in each cell of the wind region too (our procedure here takes into account cooling by the ionization, bremsstrahlung and synchrotron processes to arrive at the steady-state electron and positron distributions within each clump; see Crocker *et al.* (2007a) for details). The same extension – to still lower proton energies – allows us to also predict the lower-energy γ-ray spectrum from the CND (and also the wind region). The total γ-ray and synchrotron radio emission curves for all cells in the CND are shown as the solid (blue) curves in Figures 1 (a) and (b), respectively. Gamma-ray and radio emission by cells in the wind region is shown by the long-dashed (purple) curves in the same figures. As may be seen, the γ-ray normalized secondary synchrotron radio flux from the CND directly accounts for ~ 10 % of the observed GHz radio emission but with a rather flatter spectrum than the observation data suggest. In contrast, the wind region is modeled to produce a radio spectrum consistent with observation but with around twice the observed normalization. Given that this determination involves absolutely no fine tuning and is predicated on a fit of theoretical γ-ray emission *from a separate region* (i.e., the CND clumps) to the TeV HESS data, this is a remarkable level of agreement and we conclude that our secondary emission model can self-consistently account for both the γ-ray emission seen from the direction of the GC and the total radio emission from the wind and CND regions (i.e., a $2 \times 1'$ region centered in Sgr A*).

In Figure 1 (a) one notes that the CND γ-ray emission for the scenario above is roughly consistent with the level of emission seen from the EGRET source 3EG J1746-2851 (Mayer-Hasselwander *et al.* 1998) at the two lowest energy data points around 70 MeV. We do not claim, however, that the CND emission explains the origin of the observed γ-rays. In fact, recent studies have shown that the EGRET source excludes the GC at the 99.9% confidence level (Hooper & Dingus 2002; Pohl 2005). On the other hand, the position of the *predicted* CND emission was certainly inside the wide field of view of the EGRET instrument's GC pointings. The spectrum of 3EG J1746-2851 serves, then, as an upper limit to the allowed emission from the CND. The (blue) solid curve would seem to be just excluded. A fit to the HESS data with the additional constraint that the extrapolated γ-ray emission

obey the constraint that it be unobserved by EGRET (which we translate to the requirement that the predicted low energy gamma ray curve pass 2σ below the most constraining EGRET datum near 70 MeV) requires $X \simeq 0.8$ and the radio spectrum obtained in this case, shown as the (red) short-dashed curve in 1 (b), is statistically compatible with the radio data. The reduced χ^2 for this case is rather bad, however: 2.2 for 32 degrees of freedom. The CND γ-ray spectrum for this case is shown as the (red) short-dashed curve in 1 (a).

Also shown in Figures 1 (a) and (b) are (yellow) dot-dash curves that show, respectively, the predicted gamma-ray and radio emission for a single zone model that assumes a single power-law p population ($\sim E^{-2.3}$) tuned to match the HESS emission. With such a model one notes that, as first determined by Crocker *et al.* (2005), the low energy γ-ray curve passes well below the EGRET points. But the model predicts far too little synchrotron when compared with our full calculations that sum emission over each clump of the CND and wind regions with its own p spectrum, magnetic field and ambient hydrogen number density. This underestimation probably arises from the assumption of a 'mean' B field within the single zone model that implictly neglects the (i) relative accumulation of protons into clumps of higher magnetic field strength (where they are more strongly trapped than elsewhere) and (ii) the greater synchrotron emissivity of secondaries created in such clumps.

Finally, we have reviewed data available from observations of the GC and the CND and wind regions at other wavelengths to see whether these offer any further constraint on our model.

Given the steady-state positron production rate in our scenario we predict a 511 keV γ-ray production rate from electron-positron annihilation of $\sim 6\times10^{46}$ yr^{-1}, well inside the limit from INTEGRAL observations ($\sim 10^{50}$ yr^{-1} out to an angular radius of 8°: Knödlseder et al. (2003)

Another possible constraint is offered by hard X-ray/soft γ-ray observations. Our model predicts diffuse secondary emission at energies of 10^{4-5} eV due to both the bremsstrahlung and, dominantly, synchrotron processes. We have modeled such emission to compare it against the spectrum, at a comparable energy, of the INTEGRAL/IBIS source IGRJ17456-2901 (Belanger *et al.* 2004); we find ourselves well below the level of flux from this source.

5. Conclusions

There are several major conclusions we can draw from this study:

(1) The pre-existing data were not sufficient for a tight constraint on our predictions. New

data were acquired for this project. The compilation of data demonstrates that the black hole-induced hadronic model for the TeV gamma rays introduced in Ballantyne *et al.* (2007) is certainly consistent with the broadband emission from this process at other wavelengths.

(2) In fact, more strongly, we have also shown that, *without fine-tuning, the hadronic process may actually explain essentially all the diffuse radio emission observed from the inner few pc of the Galaxy.*

(3) The fact that in this model the protons energized by the black hole and ejected into the ISM accumulate in the magnetic fields of the CND, provides a spatial definition for where the secondaries will be active unlike, say, the primary lepton model, in which the electrons may be accelerated wherever shock fragments form in an expanding shell.

(4) The propagation calculation of Ballantyne *et al.* (2007) showed that diffusion processing by the GC magnetic field leads to a considerable spectral steepening of the injection spectrum, $\sim E^{1.5}$ requiring in turn, that the spectrum of protons injected close to Sgr A* must be very flat, $\sim\ E^{-0.75}$, in order to supply the requisite $\sim\ E^{-2.25}$ spectrum of γ-rays. This is much flatter than the $E^{-(2.1\rightarrow2.4)}$ spectrum expected from first-order Fermi acceleration. Such a hard spectrum might be created via the (second-order Fermi) stochastic acceleration mechanism. For instance, as determined by Liu *et al.* (2006) stochastic acceleration in a magnetically-dominated funnel close to the black hole could accelerate protons into a distribution as flat as E^{-1}, approaching the requisite hardness. The stochastic acceleration mechanism investigated by Becker *et al.* (2006) may also be able to produce the required spectrum. The question of whether a stochastic acceleration can be made to work in this context will be addressed elsewhere by the current authors.

(5) Finally, the hadronic scenario we have explored here may be a test bed of what is actually happening near the base of relativistic jets in more powerful sources, such as AGNs and quasars. There we would have a more difficult time discerning the various processes, because the environment is dense and chaotic. But in Sgr A*, the environment is much more sedate, with lower density, and less activity. Sgr A* does not itself produce relativistic jets that we can see. But that may simply be a consequence of the relative weakness of this process in this particular source. It may be that something like the proton injection/acceleration scenario (with subsequent propagation out to relatively large scales before final interaction) posited in our earlier paper – and whose phenomenological consequences we have explored here – is happening on a much bigger scale in the more powerful AGNs.

The authors thank Todor Stanev for producing the simulated secondary particle spectra from pp collisions exploited in this paper and Anne Green for providing the SUMSS GC 843 MHz data in numerical form. DRB is supported by the University of Arizona Theoretical

Astrophysics Program Prize Postdoctoral Fellowship. RMC gratefully acknowledges advice and assistance from Ray Protheroe. RMC is supported at the University of Adelaide by Ray Protheroe and Ron Ekers' Australian Research Council's Discovery funding scheme grant (project number DP0559991). This work was funded, in part, at the University of Arizona by NSF grant AST-0402502. The work has made use of NASA's Astrophysics Data System Abstract Service. FM is grateful to the University of Melbourne for its support (through a Sir Thomas Lyle Fellowship and a Miegunyah Fellowship).

REFERENCES

Aharonian, F.A. *et al.*, 2004, A&A, 425, 13

Aharonian, F.A. *et al.*, 2006a, Nature, 439, 695

Aharonian, F.A. *et al.*, 2006b, Phys. Rev. Lett., 97, 221102

Baganoff, F.K. *et al.*, 2003, ApJ, 591, 891

Ballantyne, D. R., Melia, F., Liu, S., & Crocker, R. M. 2007, ApJ, 657, L13

Becker, P.A., Le, T. & Dermer, C.D., 2006, ApJ, 647, 539

Belanger, G., *et al.* 2004, ApJ, 601, L163

Brogan, C., *et al.*, 2003, Astronomische Nachrichten Supplement, 324, 17

Brown, R. L., Johnston, K. J., & Lo, K. Y. 1981, ApJ, 250, 155

Crocker, R.M., Fatuzzo, M., Jokipii, J.R., Melia, F. & Volkas, R.R. 2005, ApJ, 622, 892

Crocker, R.M., *et al.*, 2007a ApJ *in press*, (astro-ph/0702045).

Crutcher, R. M. 1999, ApJ, 520, 706

Ekers, R. D., van Gorkom, J. H., Schwarz, U. J., & Goss, W. M. 1983, A&A, 122, 143

Fatuzzo, M., & Melia, F. 2003, ApJ, 596, 1035

Gopal-Krishna, & Swarup, G. 1976, Astrophys. Lett., 17, 45

Hooper, D. & Dingus, B. 2002, in the proceedings of the 34th COSPAR Scientific Assembly (astro-ph/0212509)

Jones, D.I., *et al.*, in prep., 2007.

Knödlseder, J., et al. 2003, A&A, 411, L457

LaRosa, T., *et al.*, AJ, 119, 107, 2000.

Liu, S., Melia, F., Petrosian, V. & Fatuzzo, M. 2006, ApJ, 647, 1099

Mayer-Hasselwander, H. A., *et al.* 1998, A&A, 335, 161

Melia, F., 2007, The Galactic Supermassive Black Hole, Princeton University Press

Pedlar, A., Anantharamaiah, K. R., Ekers, R. D., Goss, W. M., van Gorkom, J. H., Schwarz, U. J., & Zhao, J.-H. 1989, ApJ, 342, 769

Pohl, M. 2005, ApJ, 626, 174

Rockefeller, G., Fryer, C. L., Melia, F. & Warren, M. S. 2004, ApJ, 604, 662

Salter, C. J., Sinha, R. P., Stobie, E. B., Kerr, F. J., & Hobbs, R. W. 1988, MNRAS, 232, 407

Sofue, Y., Inoue, M., Handa, T., Tsuboi, M., Hirabayashi, H., Morimoto, M., & Akabane, K. 1986, PASJ, 38, 475

Tsuboi, M., Handa, T., Inoue, M., Ukita, N., & Takano, T. 1988, PASJ, 40, 665

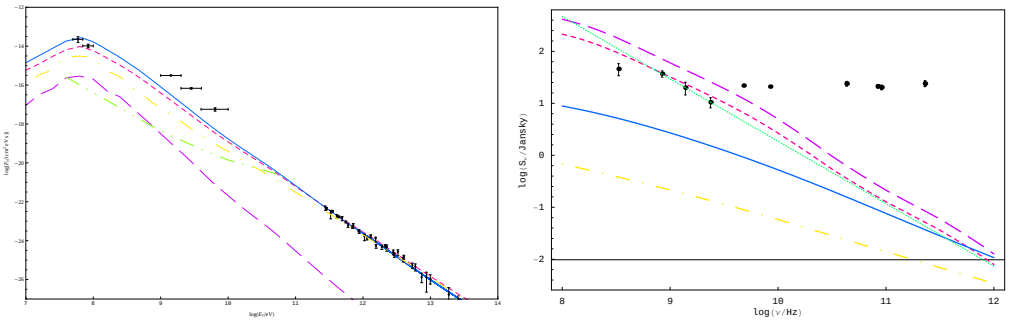

Fig. 1.— **a.** (**left**) Observed γ-ray flux data points for the GC region with theoretical spectral curves. The data points in the $\sim$ TeV range show the HESS source coincident with Sgr A*. The five lower energy data points are from the EGRET source 3EG J1746-2851. The theoretical curves are: (blue) **solid**: γ-ray spectrum from the entire CND after χ^2 fitting to the X parameter *to the HESS data only*; (red) **short dashed**: γ-ray spectrum from the entire CND after χ^2 fitting of the X parameter to the HESS data *with the additional constraint that the EGRET upper limit is obeyed*; (purple) **long dashed**: γ-ray spectrum from the wind region clumps assuming the same X value; (yellow) **dot-dash**: γ-ray spectrum for the case of a single zone (with $B = 0.35$ mG and $n_H \simeq 2.3 \times 10^5$ cm^{-3}) model and a single, power-law proton population; (green) **dot-dot-dash**: projected GLAST sensitivity for a 5 σ detection of a point-source with a $\propto E^2$ spectrum (see the GLAST website: http://www-glast.stanford.edu). **b.** (**right**) Observed radio fluxes from the CND and wind regions together with theoretical predictions for radio emission. The theoretical radio curves are: (blue) **solid**: radio emission from the **CND** region for the case that the theoretical CND γ-ray emission is optimized in X to the HESS data; (purple) **long dashed**: radio emission from the **wind** region assuming the same X value; (red) **short dashed**: radio emission from the **wind** region for the case that the theoretical CND γ-ray emission is optimized in X to the HESS data *with the additional constraint that the EGRET upper limit is obeyed*; (green) **dotted** curve: simple power law fit to 843, 1384, and 2368 MHz flux points.